

On Aggregation Queries over Predicted Nearest Neighbors

Carrie Wang
The University of Hong Kong
Hong Kong SAR, China
carrie07@connect.hku.hk

Laks V. S. Lakshmanan
The University of British Columbia
Vancouver, Canada
laks@cs.ubc.ca

Sihem Amer-Yahia
CNRS, Univ. Grenoble Alpes
Grenoble, France
sihem.amer-yahia@univ-grenoble-alpes.fr

Reynold Cheng
The University of Hong Kong
Hong Kong SAR, China
ckcheng@cs.hku.hk

ABSTRACT

We introduce Aggregation Queries over Nearest Neighbors (AQNNs), a novel type of aggregation queries over the *predicted* neighborhood of a designated object. AQNNs are prevalent in modern applications where, for instance, a medical professional may want to compute *the average systolic blood pressure of patients whose predicted condition is similar to a given insomnia patient*. Since prediction typically involves an expensive deep learning model or a human expert, we formulate query processing as the problem of returning an approximate aggregate by combining an expensive oracle and a cheaper model (e.g. a simple ML model) to compute the predictions. We design the Sampler with Precision-Recall in Target (SPR_{inT}) framework for answering AQNNs. SPR_{inT} consists of sampling, nearest neighbor refinement, and aggregation, and is tailored for various aggregation functions. It enjoys provable theoretical guarantees, including bounds on sample size and on error in approximate aggregates. Our extensive experiments on medical, e-commerce, and video datasets demonstrate that SPR_{inT} consistently achieves the lowest aggregation error with minimal computation cost compared to its baselines. Scalability results show that SPR_{inT}'s execution time and aggregation error remain stable as the dataset size increases, confirming its suitability for large-scale applications.

PVLDB Reference Format:

Carrie Wang, Sihem Amer-Yahia, Laks V. S. Lakshmanan, and Reynold Cheng. On Aggregation Queries over Predicted Nearest Neighbors. PVLDB, 14(1): XXX-XXX, 2020.
doi:XX.XX/XXX.XX

PVLDB Artifact Availability:

The source code, data, and/or other artifacts have been made available at <https://github.com/Carrieww/AQNNs>.

1 INTRODUCTION

Many applications today require to compute aggregations efficiently over the neighborhood of a designated object. When the neighborhood is not known, it needs to be predicted. That is the case for queries commonly asked by medical professionals such

This work is licensed under the Creative Commons BY-NC-ND 4.0 International License. Visit <https://creativecommons.org/licenses/by-nc-nd/4.0/> to view a copy of this license. For any use beyond those covered by this license, obtain permission by emailing info@vldb.org. Copyright is held by the owner/author(s). Publication rights licensed to the VLDB Endowment.
Proceedings of the VLDB Endowment, Vol. 14, No. 1 ISSN 2150-8097.
doi:XX.XX/XXX.XX

Data Point (total 10 points)	Systolic Blood Pressure	Ground Truth
NN1	128	AVG = $\frac{128 + 132 + 125}{3}$ = 128.3
NN2	132	VAR = $\frac{(128-128.3)^2 + (132-128.3)^2 + (125-128.3)^2}{3}$ = 8.22
NN3	125	SUM = 128 + 132 + 125 = 385
False NN4	160	PCT = 3/10

Case 1: Low Precision (Add NN4) Precision = 3/4, Recall = 1	Case 2: Low Recall (Miss NN2) Precision = 1, Recall = 2/3
AVG = 136.25 SUM = 545	AVG = 126.5 SUM = 253
VAR = 194.1875 PCT = 4/10	VAR = 2.25 PCT = 2/10

Figure 1: A numerical example showing how precision and recall affects error in AQNN results.

as computing *the average systolic blood pressure of patients whose predicted condition is similar to a designated insomnia patient* [20]. We call such queries AQNNs, or Aggregation Queries over Nearest Neighbors. AQNNs extend the well-known Fixed-Radius Near Neighbor (FRNN) queries [4] with *prediction* and *aggregation*. The exact evaluation of AQNNs is costly as it relies on a predictive model, a.k.a. an oracle [10, 23, 25], to determine the neighborhood of the input object and compute an aggregated value. In this paper, we formulate and solve the problem of evaluating AQNNs by seeking an approximate aggregate result that leverages both an expensive oracle and a cheaper predictive model, namely a proxy model [2, 10, 22, 27], to compute the predictions.

Objectives and Challenges. Answering an AQNN approximately requires addressing two key objectives: (O1) ensuring low error between the approximate and true aggregates, and (O2) minimizing computational cost. The main challenge for O1 is to ensure that the retrieved nearest neighbors are both correct and complete, with high likelihood, formally stated as achieving high precision and recall. For example, as illustrated in Fig. 1, both low-precision (Case 1) and low-recall (Case 2) scenarios introduce aggregation error. Additionally, Case 1 results in a significantly larger error for AVG and VAR. Assuming the value distributions of the true nearest neighbors and non-nearest neighbors are consistent within themselves but differ from each other, precision is generally more important than recall for *value-based* aggregation functions, including AVG, VAR,

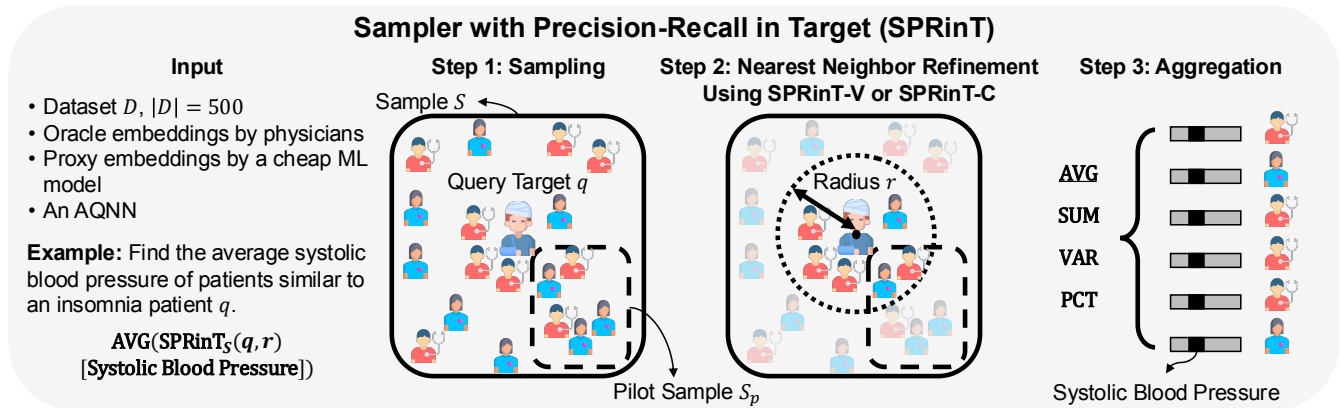


Figure 2: Overview of the SPRinT framework for answering AQNNs.

and SUM, as it prevents outliers and noisy values from distorting AQNN results. Therefore, for value-based aggregation functions, we aim to maximize $F\beta$ score, a weighted harmonic mean of precision and recall, for the retrieved nearest neighbors. On the other hand, *count-based* aggregation functions, such as percentage (PCT), are more sensitive to imbalances between precision and recall. For instance, in Fig. 1, missing NN2 while adding False NN4 results in both precision and recall equaling $2/3$, which does not affect the approximate percentage. Hence, to reduce error in count-based aggregation functions, we aim to equalize precision and recall, i.e. equalizing false positives and false negatives. This prevents systematic over- or under-estimation of the aggregate.

Achieving **O2**, however, inherently conflicts with **O1**. First, predicting nearest neighbors relies on distances derived from oracle embeddings, which are highly accurate but computationally expensive. In contrast, proxy embeddings are computationally cheaper but inaccurate, leading to lower precision and recall when predicting nearest neighbors, and hence introducing larger aggregation error [2, 10, 22, 27]. Second, verifying precision and recall for selected nearest neighbors requires identifying true nearest neighbors, which depends on expensive oracle embeddings. This exacerbates the trade-off between **O1** and **O2**. *Our overarching goal is to strike a balance between cost and error by optimizing precision and recall in a manner that is tailored to different aggregation functions.*

Technical Contributions. We design *Sampler with Precision-Recall in Target* (SPRinT), our framework for answering AQNNs. SPRinT consists of three steps: (1) sampling, (2) nearest neighbor refinement, and (3) aggregation. To address **O2**, we first reduce computational cost by drawing a random sample S from D . The random sampler preserves data distribution, which ensures that the approximate aggregates in S reflect the true aggregates in D . Additionally, we draw a pilot sample S_p from S to restrict the use of the expensive oracle to S_p , while employing a computationally efficient proxy for all data in S . The function of the pilot sample is twofold: (1) enabling direct verification of precision and recall using oracle embeddings in S_p , which we can use to monitor the precision and recall performance of the proxy in S (**O1**), and (2) refining the retrieved neighbor set. We develop SPRinT-V and SPRinT-C, two algorithms that cater to

value- and count-based aggregation functions, respectively. SPRinT-V optimizes the $F\beta$ score by dynamically adjusting precision and recall targets to minimize the aggregation error. SPRinT-C equalizes precision and recall targets in S to ensure the number of selected nearest neighbors is neither over- nor under-estimated.

Furthermore, we derive theoretical bounds on the minimum required sample size and on the minimum required pilot sample size, showing that they are both independent of the dataset size. This scalability enables our framework to handle very large datasets. In addition, we present two theorems that establish error bounds between the approximate and true aggregates for AVG and PCT.

Empirical Findings. We run extensive experiments on a variety of datasets (medical, social media, and video), and we measure relative aggregation error (RE) and response time. Our findings reveal that SPRinT-V consistently achieves the lowest RE across all datasets compared with baselines under the same predefined oracle cost, owing to its ability to attain the highest $F\beta$ scores. We also observe that both the sample and pilot sample sizes must be sufficiently large to ensure reliable estimation of precision, recall, and the $F\beta$ score, which are critical for accurate approximation of aggregates. Furthermore, the radius of an AQNN affects the number of true nearest neighbors and, consequently, the RE. Specifically, when the proportion of true nearest neighbors is $\leq 5\%$, larger sample and pilot sample sizes are required; otherwise, the RE of our proposed method cannot be reliably guaranteed. Interestingly, the reliance of SPRinT-V and SPRinT-C on sampled data makes them highly scalable as they are independent from the dataset size. Our results position the SPRinT framework as an excellent solution for large-scale applications requiring neighborhood aggregation where accuracy is critical (e.g., medical). This is further demonstrated on a key application of AQNNs – one-sample hypothesis testing where SPRinT-V and SPRinT-C consistently achieve the highest accuracy for t-tests and proportion z-tests while exhibiting low costs.

2 PROBLEM STUDIED

We first present Fixed-Radius Near Neighbor (FRNN) queries and then formalize Aggregation Queries over Nearest Neighbors (AQNNs) that build on them. We then state our problem.

2.1 Nearest Neighbor Queries

We build on generalized Fixed-Radius Near Neighbor (FRNN) queries [4]. Given a dataset D , a query object q , a radius r , and a distance function $dist$, a generalized FRNN query retrieves all nearest neighbors of q within radius r . More formally:

$$NN_D(q, r) = \{x \in D \mid dist(x, q) \leq r\},$$

where x is any data point in D and $dist(x, q)$ denotes the distance between them. We use $|NN_D(q, r)|$ to denote the neighborhood size of q . As shown in Fig. 2, given a radius r and a target patient q , patients in the dotted circle are nearest neighbors, and the neighborhood size is 6.

2.2 Aggregation Queries over Nearest Neighbors

Given an FRNN query object q in dataset D , a radius r , and an attribute $attr$, an Aggregation Query over Nearest Neighbors (AQNN) is defined as:

$$agg(NN_D(q, r)[attr])$$

where agg is an aggregation function, such as AVG, SUM, and PCT, and $NN_D(q, r)[attr]$ denotes the bag of values of attribute $attr$ of all FRNN results of q within radius r .

An AQNN expresses aggregation operations to capture key insights about the neighborhood of a query object. For example, AVG can be used to reflect the average heart rate or systolic blood pressure of patients in the neighborhood, providing a measure of typical health conditions. SUM is useful for assessing cumulative effects, such as the total cost of treatments in the neighborhood that instructs public policy in terms of health. Similarly, PCT can be used to find the proportion of patients in the neighborhood of a patient of interest, relative to the population in the dataset.

Fig. 2 illustrates an example of an AQNN: “Find the average systolic blood pressure of patients similar to an insomnia patient q ”. The aggregation function is AVG and the target attribute of interest is systolic blood pressure. Exact query evaluation requires consulting physicians (or predicting embeddings by an expensive machine learning model) for all 500 patients in D and calculate q ’s nearest neighbors wrt r [20]. We refer to such highly accurate but computationally expensive models as *oracle models*, denoted as O , including deep learning models trained on domain-specific data or human expert annotations [27]. Using oracle models is very expensive [10, 23, 33]. To address that, we seek an approximate solution by *proxy models*, denoted as P , that are at least one order of magnitude cheaper than oracle models. In the example, if consulting physicians for one patient incurs one cost unit, calling a cheap machine learning model instead incurs at most 0.1 cost unit. Once the similar patients are identified, their systolic blood pressure values are averaged and returned as output. The use of a proxy model may reduce the accuracy of the neighborhood prediction and hence, we should judiciously call oracle and proxy models to minimize the error of aggregate results.

Note that the values of the target attribute $attr$ are *not* predicted but are instead known quantities.

Table 1: Table of Notations

Notation	Description
D	the dataset
O	oracle model
P	proxy model
q	query point
S	random sample of D with size s
ON_D	oracle neighbors in D
ON_S	oracle neighbors in S
$SPRinT_S$	SPRinT neighbors in S
S_p	pilot sample in S with size s_p
t^*	optimal recall target
R_S	recall in S
P_S	precision in S
$F\beta_S$	$F\beta$ score in S

2.3 Problem Statement

Given an AQNN, our goal is to return an approximate aggregate result by leveraging both oracle and proxy models while reducing error and cost.

3 OUR SOLUTION

In this section, we first discuss our objectives and challenges (§ 3.1), then describe the Sampler with Precision-Recall in Target (SPRinT) framework for answering AQNNs (§ 3.2). For value- and count-based aggregation functions, we introduce SPRinT-V (§ 3.2.1) and SPRinT-C (§ 3.2.2), which respectively maximize $F\beta$ score and equalize recall and precision. We then theoretically analyze our framework (§ 3.3) where we derive error bounds on approximate aggregates and the minimal sample and pilot sample size required to ensure reliable aggregation approximation.

3.1 Objectives and Challenges

Recall the objectives in answering an AQNN: **(O1)** ensure a low approximation error and **(O2)** minimize computational cost.

To achieve **O1** for value-based aggregation functions, the key challenge lies in ensuring that the retrieved nearest neighbors are both correct and complete, with high likelihood, formally expressed as achieving high precision and recall. Precision measures the proportion of retrieved neighbors that are correct, while recall measures the proportion of true nearest neighbors that are retrieved, which is essential for completeness. As shown in Fig. 1, both low-precision (Case 1) and low-recall (Case 2) scenarios introduce aggregation error. However, precision and recall often conflict. A higher precision may exclude true neighbors, lowering recall, whereas a higher recall may introduce incorrect neighbors, reducing precision. Additionally, Case 1 results in a significantly larger error for AVG and VAR. Assuming the value distributions of the true nearest neighbors and non-nearest neighbors are consistent within themselves but differ from each other, precision is generally more important than recall for *value-based* aggregation functions, including AVG, VAR, and SUM, as it prevents outliers and noisy values from distorting AQNN results. Therefore, striking the right balance between these two metrics is key to reducing error between the approximate and true aggregate in D . On the other hand, count-based aggregation functions are more sensitive to the imbalances between precision

and recall. If the false positives and false negatives are equal, we can prevent systematic over- or under-estimation of the aggregate for count-based aggregation functions.

Achieving **O2**, however, inherently conflicts with **O1**. First, distances derived from oracle embeddings are highly accurate, often yielding the highest precision and recall for nearest neighbor selection, but are computationally expensive. In contrast, proxy embeddings are computationally cheaper but reduce the accuracy of neighborhood prediction, leading to lower precision and recall. Second, verifying precision and recall for selected nearest neighbors requires identifying true nearest neighbors, which depends on expensive oracle embeddings. This exacerbates the trade-off between two objectives.

Our overarching goal is to strike a balance between cost and error by optimizing precision and recall in a manner that is tailored to different aggregation functions.

To address **O1** for *value-based* aggregation functions, we propose to optimize *precision and recall* by maximizing $F\beta$ score, a weighted harmonic mean of precision and recall, for the retrieved nearest neighbors. Here, $\beta < 1$ weights recall lower than precision while $\beta > 1$ weights recall higher than precision. On the other hand, *count-based* aggregation functions require a different approach. For these functions, accurately approximating the number of nearest neighbors is critical to ensure low error. Hence, equalizing precision and recall is essential to prevent systematic over- or under-estimation. For instance, when recall is higher than precision, false positives are higher than false negatives. It results in an over-estimation of the number of nearest neighbors because too many irrelevant neighbors are included. Conversely, when precision is higher than recall, too many true neighbors are missed, leading to an under-estimation. Thus, achieving **O1** entails optimizing both precision and recall in sync. However, existing literature [10, 23] typically focuses on optimizing either precision or recall in isolation, and does not optimize both or achieve a balance thereof.

To address **O2**, we first draw a random sample to reduce the computational cost. Random sampling is effective at preserving the overall distribution of the data by ensuring that each data point in D has an equal probability of being selected. As a result, the nearest neighbor found in the sample S can serve as an effective approximation for the nearest neighbor in D , enabling us to approximate the aggregate over D without processing the entire dataset. To further reduce the cost, we additionally draw a pilot sample S_p from S and only call the expensive oracle on the data in S_p , while using a computationally efficient proxy on all data in S . The pilot sample serves two key purposes when finding nearest neighbors in S . First, with oracle embeddings for data in S_p , we can directly verify the precision and recall within this subset. Due to the properties of the random sampler (formal proof in Appendix 7.1), the precision and recall measured in S_p reliably approximate those in the full sample S . Consequently, we can monitor and optimize the precision and recall in S based on their performance in S_p (**O1**). Second, the true nearest neighbors in S_p can be used to refine the retrieved neighbor set in S . This refinement further improves the $F\beta$ score and equalizes precision and recall for value- and count-based aggregation functions, respectively (**O1**).

Algorithm 1 SPRinT-V

```

1: Input:  $S, S_p, O, P, q, \beta, \omega_V$ 
2: Output: SPRinT $_S$ 
3:  $t_{\min} \leftarrow 0, t_{\max} \leftarrow 1$ 
4: while  $t_{\max} - t_{\min} > \omega_V$  do
5:    $t_1 \leftarrow t_{\min} + \frac{t_{\max} - t_{\min}}{3}, t_2 \leftarrow t_{\max} - \frac{t_{\max} - t_{\min}}{3}$ 
6:    $NN(t_1) \leftarrow \text{PQE-PT}(S_p, O, P, q, t_1)$ 
7:    $NN(t_2) \leftarrow \text{PQE-PT}(S_p, O, P, q, t_2)$ 
8:    $F\beta_{S_p}(t_1) \leftarrow (1 + \beta^2) \frac{P_{S_p}(t_1)R_{S_p}(t_1)}{\beta^2 P_{S_p}(t_1) + R_{S_p}(t_1)}$ 
9:    $F\beta_{S_p}(t_2) \leftarrow (1 + \beta^2) \frac{P_{S_p}(t_2)R_{S_p}(t_2)}{\beta^2 P_{S_p}(t_2) + R_{S_p}(t_2)}$ 
10:  if  $F\beta_{S_p}(t_1) > F\beta_{S_p}(t_2)$  then
11:     $t_{\max} \leftarrow t_2$ 
12:  else
13:     $t_{\min} \leftarrow t_1$ 
14:  end if
15: end while
16:  $t^* \leftarrow (t_{\min} + t_{\max})/2$ 
17: return PQE-PT( $S, O, P, q, t^*$ )

```

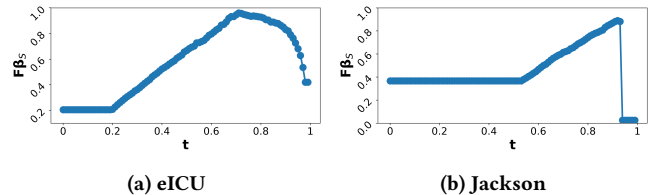


Figure 3: F1 score curves for eICU (a) and Jackson (b) datasets

3.2 The SPRinT Framework

Fig. 2 illustrates SPRinT, our framework for answering AQNNs. It consists of three main steps: (1) sampling, (2) nearest neighbor refinement, and (3) aggregation. First, given a dataset D and a desired sample size s , we draw a random sample S of size s using a random sampler. Since $s \ll |D|$, this step significantly reduces the overall computational cost (**O2**). In the second step, we approximate AQNN results on S using a combination of proxy and oracle embeddings. From S , we randomly draw a smaller pilot sample S_p of size s_p ; while proxy models are applied to all data in S , the expensive oracle models are invoked only on data in S_p . It further reduces the oracle cost (**O2**). By computing precision and recall on S_p , we can monitor the performance of different nearest neighbor selection strategies in S to verify whether we achieve the maximum $F\beta$ score or equal precision and recall (**O1**). In the third step, after selecting the nearest neighbors in S , we apply the specified aggregation function (e.g., AVG, SUM, PCT) to the target attribute of these neighbors. The final output is the approximate aggregate.

3.2.1 SPRinT-V. For value-based aggregation functions, we propose SPRinT-V to find nearest neighbors in the second step. Our goal is to identify neighbors which maximize the $F\beta$ score in S with high probability. However, directly optimizing the $F\beta$ score is challenging because it depends non-linearly on both precision and recall, with improvements in one often coming at the expense of the other.

Instead, we leverage the insight that if a nearest neighbor search algorithm can *guarantee* one metric while *maximizing* another, it can effectively navigate this trade-off. PQE-PT and PQE-RT are state-of-the-art approaches that meet this requirement by ensuring that the selected neighbors achieve a given precision (resp. recall) target with high probability while maximizing recall (resp. precision) [10]. Since accurate aggregate estimates in value-based functions are more sensitive to precision, where false positives can significantly distort the result, we favor PQE-PT, which prioritizes achieving a precision target before maximizing recall, over PQE-RT. In practical settings, as illustrated in Fig. 3, the $F\beta$ score is found to be unimodal when using PQE-PT. This unimodality allows us to efficiently search for the optimal $F\beta$ score via ternary search. Rather than directly specifying an $F\beta$ score target, we iteratively explore different precision targets until we find the optimal precision target t^* that maximizes the $F\beta$ score of the selected nearest neighbors. Consequently, we integrate PQE-PT as a subroutine in SPRinT-V to identify the nearest neighbors in S .

As shown in Algorithm 1, SPRinT-V takes as inputs S, S_p, O, P, q, β , and a tolerance ω_V and outputs the SPRinT neighbors in S . The algorithm first initializes the range of precision targets with $t_{\min} = 0$ and $t_{\max} = 1$ (Line 3) and iteratively narrows this range until $t_{\max} - t_{\min} < \omega_V$ (Line 4). In each iteration, two candidate thresholds, t_1 and t_2 , are calculated by dividing the range into thirds (Line 5). The PQE-PT subroutine is then called with t_1 and t_2 to retrieve the nearest neighbors in S_p (Lines 6-7). Using these selected neighbors and the oracle neighbors in S_p , the algorithm computes precision (P_{S_p}), recall (R_{S_p}), and $F\beta$ scores for both t_1 and t_2 (Lines 8-9). Next, SPRinT-V updates the search range by retaining the more promising region of the precision target (Lines 10-14). Once the search range converges, t^* is computed as the midpoint of t_{\min} and t_{\max} (Line 16). Finally, PQE-PT is called one last time with t^* to retrieve the SPRinT neighbors in S (Line 17), which are then used to compute the aggregation of an AQNN query.

3.2.2 SPRinT-C . For count-based aggregation functions, we propose SPRinT-C to find nearest neighbors. Similar to SPRinT-V , SPRinT-C leverages PQE-PT to iteratively adjust the precision target until the precision of the SPRinT neighbors in S_p matches the recall. The intuition is that balancing false positives and false negatives leads to an unbiased estimation of the proportion of nearest neighbors. Specifically, we define the approximated proportion as:

$$\widehat{\text{PCT}}_S = \frac{|\text{SPRinT}_S|}{s} = \frac{|(\text{SPRinT}_S \cap \text{ON}_S) \cup (\text{SPRinT}_S \setminus \text{ON}_S)|}{s} \quad (1)$$

where SPRinT_X (resp. ON_X) denotes the nearest neighbors found by SPRinT (resp. true nearest neighbors) in dataset $X, X \in \{S, D\}$. When the number of false positives ($|\text{SPRinT}_S \setminus \text{ON}_S|$) equals the number of false negatives ($|\text{ON}_S \setminus \text{SPRinT}_S|$), $\widehat{\text{PCT}}_S$ accurately reflects PCT_S . This condition is satisfied when precision equals recall. Formally, the recall and precision of the SPRinT neighbors in S are: $R_S = \frac{|\text{SPRinT}_S \cap \text{ON}_D|}{|\text{ON}_S|}$, and $P_S = \frac{|\text{SPRinT}_S \cap \text{ON}_D|}{|\text{SPRinT}_S|}$. By setting $P_S = R_S$, we can infer $|\text{SPRinT}_S \setminus \text{ON}_S| = |\text{ON}_S \setminus \text{SPRinT}_S|$, i.e., the numbers of false positives and false negatives are balanced. Hence, $\widehat{\text{PCT}}_S$ provides an unbiased estimation of PCT_S .

As shown in Algorithm 2, SPRinT-C takes the same inputs as SPRinT-V and outputs the SPRinT neighbors in S . Since there is an

Algorithm 2 SPRinT-C

```

1: Input:  $S, S_p, O, P, q, \omega_C$ 
2: Output:  $\text{SPRinT}_S$ 
3:  $t_{\min} \leftarrow 0, t_{\max} \leftarrow 1$ 
4: while  $|R_{S_p} - P_{S_p}| > \omega_C$  do
5:    $t^* \leftarrow \frac{t_{\min} + t_{\max}}{2}$ 
6:    $NN \leftarrow \text{PQE-PT}(S_p, O, P, q, t^*)$ 
7:    $R_{S_p} \leftarrow \frac{|NN \cap \text{ON}_D \cap S_p|}{|\text{ON}_D \cap S_p|}, P_{S_p} \leftarrow \frac{|NN \cap \text{ON}_D \cap S_p|}{|NN \cap S_p|}$ 
8:   if  $P_{S_p} \leq R_{S_p}$  then
9:      $t_{\min} \leftarrow t^*$ 
10:  else
11:     $t_{\max} \leftarrow t^*$ 
12:  end if
13: end while
14: return  $\text{PQE-PT}(S, O, P, q, t^*)$ 

```

inverse relationship between precision and recall, where a higher precision target leads to a lower recall, a binary search is employed to find the optimal precision target t^* which equalizes precision and recall. SPRinT-C initializes the search range with $t_{\min} = 0$ and $t_{\max} = 1$ (Line 3) and iteratively narrows this range until the difference between the recall R_{S_p} and precision P_{S_p} in the pilot sample is within a tolerance ω_C (Line 4). In each iteration, a candidate precision target is set to the midpoint of the current range (Line 5). The PQE-PT subroutine is then invoked to retrieve the nearest neighbors in S_p (Line 6). The corresponding R_{S_p} and P_{S_p} are then computed based on the oracle-determined true neighbors in S_p (Line 7), and the search range is updated accordingly (Lines 8-12). Finally, once the optimal t^* is determined, PQE-PT is called with t^* to retrieve the SPRinT neighbors in S (Line 14).

Time Complexity. The time complexity for both algorithms is dominated by the invocation of PQE-PT, which has a time complexity of $O(s^2 \log(s))$ [10], $s = |S|$ being the sample size. During the search for the optimal t^* , SPRinT-V performs a ternary search and SPRinT-C performs a binary search, requiring $O(\log(1/\omega_V))$ and $O(\log(1/\omega_C))$ iterations¹. Assuming $\omega_C = \omega_V = \omega^*$, the overall time complexity is $O(\log(1/\omega^*)s^2 \log(s))$. Evaluating precision and recall over S_p introduces another linear term $O(s_p)$. But since $s_p \ll s$, its impact becomes negligible in the asymptotic analysis. Therefore, SPRinT-V and SPRinT-C scale quadratically with s (up to logarithmic factors), and the number of iterations needed for convergence depends only logarithmically on ω^* .

3.3 Theoretical Analysis

In this section, we establish results on the error bounds of AVG and PCT achieved by SPRinT-V and SPRinT-C , respectively. Also, we derive the minimum sample and pilot sample size required to achieve the bound.

THEOREM 1. *Let $\widehat{\text{AVG}}_S$ be the approximate aggregate returned by SPRinT-V . Given a target error bound $\omega = \omega_D + \omega_S$, and a confidence*

¹Ternary search uses \log_3 while binary search uses \log_2 . But for asymptotic analysis, these differences are absorbed in the constant factors.

level of $1 - \alpha$, the approximation error satisfies:

$$\Pr \left[\left| \overline{\text{AVG}}_S - \text{AVG}_D \right| \leq \omega \right] \geq 1 - \alpha, \quad (2)$$

provided:

$$s \geq \frac{(b-a)^2 \ln(2/\alpha)}{2|ON_S| \omega_D^2}, \quad (3)$$

$$s_p \geq \frac{8L^2(b-a)^2 \ln(4/(\alpha+1))}{|ON_S|^2 \omega_S^2}, \quad (4)$$

where $L = \max\{1 + \beta^2, \frac{1+\beta^2}{\beta^2}\}$.

PROOF. We begin by bounding the deviation $|\text{AVG}_D - \text{AVG}_S|$. Let $x[\text{attr}]$ denote the value of attribute attr for an object $x \in D$. For a set $X \subseteq D$, the average value of attr is

$$\text{AVG}_X = \frac{1}{|ON_X(q, r)|} \sum_{x_i \in ON_X(q, r)} x_i[\text{attr}], \quad (5)$$

where $ON_X(q, r)$ is the set of oracle neighbors of q in X within radius r . When X is D (resp. a random sample $S \subset D$), AVG_X is the true (resp. sample) average. Suppose that each $x_i[\text{attr}]$ is bounded, i.e., $x_i[\text{attr}] \in [a, b]$, for some finite $a, b \in \mathbb{R}$.² Applying Hoeffding's inequality [14, 31], the probability that AVG_S deviates from AVG_D by more than a given error $\omega_D > 0$ is

$$\Pr \left[|\text{AVG}_S - \text{AVG}_D| \geq \omega_D \right] \leq 2 \exp \left(-\frac{2|ON_S| \omega_D^2}{(b-a)^2} \right), \quad (6)$$

showing as $|ON_S|$ increases, the probability of a significant deviation between the sample and true averages decreases exponentially.

For a given confidence level $(1 - \alpha)$ (e.g., $\alpha = 0.05$ for a 95% confidence interval), to guarantee $\Pr \left[|\text{AVG}_S - \text{AVG}_D| \leq \omega_D \right] \geq 1 - \alpha$, by Eq. (6), the minimum sample size required to achieve the desired error margin ω_D w.h.p. is:

$$s \geq \frac{(b-a)^2 \ln \left(\frac{2}{\alpha} \right)}{2|ON_S| \omega_D^2}. \quad (7)$$

Next, we bound the deviation $|\overline{\text{AVG}}_S - \text{AVG}_S|$, which can be decomposed into two terms:

$$\begin{aligned} |\overline{\text{AVG}}_S - \text{AVG}_S| &\leq |1/|\text{SPRinT}_S| \cdot \sum_{x_i \in \text{SPRinT}_S} x_i[\text{attr}] \\ &\quad - 1/|\text{SPRinT}_S \cap ON_S| \cdot \sum_{x_i \in \text{SPRinT}_S \cap ON_S} x_i[\text{attr}] \\ &\quad + |1/|\text{SPRinT}_S \cap ON_S| \cdot \sum_{x_i \in \text{SPRinT}_S \cap ON_S} x_i[\text{attr}] \\ &\quad - 1/|ON_S| \cdot \sum_{x_i \in ON_S} x_i[\text{attr}] \end{aligned} \quad (8)$$

where the first term measures the error introduced by false positives ($x_i \in \text{SPRinT}_S \setminus ON_S$), while the second term captures the error from false negatives ($x_i \in ON_S \setminus \text{SPRinT}_S$). Since each false positive or false negative contributes at most $(b-a)/|ON_S|$, we bound the total error as:

$$\begin{aligned} |\overline{\text{AVG}}_S - \text{AVG}_S| &\leq \frac{(b-a)}{|ON_S|} \left[(1 - P_S) + (1 - R_S) \right] \\ &\leq \frac{2(b-a)}{|ON_S|} (1 - F\beta_S). \end{aligned} \quad (9)$$

²E.g., human systolic blood pressure typically falls in the range [70, 200] mmHg. For healthy individuals, the normal range is [90, 120] mmHg.

The last inequality follows from the fact that for positive numbers the harmonic mean is always upper bounded by the arithmetic mean, i.e., $F\beta_S \leq (P_S + R_S)/2$.

SPRinT-V maximizes the $F\beta_{S_p}$ in the refinement step (Algorithm 1). Applying Hoeffding's inequality (details in Appendix § 7.1), we establish probabilistic bounds on the deviations in precision and recall:

$$\Pr \left[|P_{S_p} - P_S| \geq \gamma/2 \right] \leq \min\{1, 2 \exp(-2s_p(\gamma/2)^2)\}, \quad (10)$$

$$\Pr \left[|R_{S_p} - R_S| \geq \gamma/2 \right] \leq \min\{1, 2 \exp(-2s_p(\gamma/2)^2)\}, \quad (11)$$

where $\gamma > 0$ is an error term. Since $f(P, R) := F\beta$ is differentiable and continuous, we apply the mean value theorem to bound $|F\beta_{S_p} - F\beta_S|$:

$$\begin{aligned} |F\beta_{S_p} - F\beta_S| &= |f(P_{S_p}, R_{S_p}) - f(P_S, R_S)| \\ &\leq \left| \frac{\partial f}{\partial P} \right| |P_{S_p} - P_S| + \left| \frac{\partial f}{\partial R} \right| |R_{S_p} - R_S| \\ &\leq L(|P_{S_p} - P_S| + |R_{S_p} - R_S|), \end{aligned} \quad (12)$$

where $L = \max\left(1 + \beta^2, \frac{1+\beta^2}{\beta^2}\right)$ is the Lipschitz constant of $F\beta$ with respect to precision and recall. By Eq. (10) and (11), we get:

$$\begin{aligned} \Pr \left[|P_{S_p} - P_S| + |R_{S_p} - R_S| \leq \frac{\gamma}{L} \right] &\geq \Pr \left[|P_{S_p} - P_S| \leq \frac{\gamma}{2L} \right] \\ &\quad + \Pr \left[|R_{S_p} - R_S| \leq \frac{\gamma}{2L} \right] \\ \text{So, } \Pr \left[|F\beta_{S_p} - F\beta_S| \leq \gamma \right] &\geq 2 - 2 \min\{1, 2 \exp(-2s_p(\frac{\gamma}{2L})^2)\}. \end{aligned} \quad (13)$$

Under a $(1 - \alpha)$ confidence interval and an error margin ω_S , by Eq. (9), for the following guarantee to hold:

$$\Pr \left[\left| \overline{\text{AVG}}_S - \text{AVG}_S \right| \leq \omega_S \right] \geq 1 - \alpha \quad (14)$$

the minimum required pilot sample size should satisfy:

$$\begin{aligned} s_p &\geq \frac{8L^2(b-a)^2 \ln(4/(\alpha+1))}{\left[|ON_S| \omega_S - 2(b-a)(1 - F\beta_{S_p}) \right]^2} \\ &\geq \frac{8L^2(b-a)^2 \ln(4/(\alpha+1))}{|ON_S|^2 \omega_S^2}. \end{aligned} \quad (15)$$

The theorem follows from Eq. (7) and (15). \square

THEOREM 2. Let $\overline{\text{PCT}}_S$ be the approximate aggregate returned by SPRinT-C . Given a target error bound $\omega = \epsilon + \omega'_D$ and confidence level $1 - \alpha$, the approximation error satisfies:

$$\Pr \left[\left| \overline{\text{PCT}}_S - \text{PCT}_D \right| \leq \omega \right] \geq 1 - \alpha, \quad (16)$$

provided:

$$s \geq \frac{\ln(2/\alpha)}{2\omega'_D}, \quad (17)$$

$$s_p \geq \frac{2 \ln(4/(\alpha+1))}{(\epsilon - \omega_C)^2}, \quad (18)$$

where $\omega_C \geq |R_{S_p} - P_{S_p}|$ is the threshold used by SPRinT-C .

PROOF. We first bound the deviation $|\text{PCT}_D - \text{PCT}_S|$. Similarly to the proof in Theorem 1, given an confidence level $(1 - \alpha)$, to guarantee $\Pr [|\text{PCT}_S - \text{PCT}_D| \leq \omega'_D] \geq 1 - \alpha$, the minimum sample size required to achieve a desired error margin $\omega'_D > 0$ is:

$$s \geq \frac{\ln(2/\alpha)}{2\omega'_D}. \quad (19)$$

We then bound the deviation $|\widetilde{\text{PCT}}_S - \text{PCT}_S|$. From Eq. (1), we have:

$$|\widetilde{\text{PCT}}_S - \text{PCT}_S| = \frac{||\text{SPRinT}_S \setminus \text{ON}_S| - |\text{ON}_S \setminus \text{SPRinT}_S||}{s}. \quad (20)$$

The deviation is determined by the count difference between false positives ($|\text{SPRinT}_S \setminus \text{ON}_S|$) and false negatives ($|\text{ON}_S \setminus \text{SPRinT}_S|$).

Using the triangle inequality, we can bound $|\text{P}_S - \text{R}_S|$ as:

$$|\text{P}_S - \text{R}_S| \leq |\text{P}_S - \text{P}_{S_p}| + |\text{R}_S - \text{R}_{S_p}| + |\text{P}_{S_p} - \text{R}_{S_p}| \quad (21)$$

$$|\text{P}_S - \text{R}_S| \leq |\text{P}_S - \text{P}_{S_p}| + |\text{R}_S - \text{R}_{S_p}| + \omega_C. \quad (22)$$

The second inequality follows by applying the stopping condition enforced by Algorithm 2, namely $|\text{P}_{S_p} - \text{R}_{S_p}| \leq \omega_C$.

Applying Hoeffding’s inequality, the probability that $|\text{P}_S - \text{R}_S|$ exceeds an error term $\epsilon > 0$ is bounded by:

$$\Pr [|\text{P}_S - \text{R}_S| \leq \epsilon] \geq \Pr \left[|\text{P}_S - \text{P}_{S_p}| + |\text{R}_S - \text{R}_{S_p}| \leq \epsilon - \omega_C \right] \quad (23)$$

$$\geq 2 - 2 \min\left\{1, 2 \exp\left(-\frac{sp(\epsilon - \omega_C)^2}{2}\right)\right\}. \quad (24)$$

Since the deviation in P_S and R_S directly translates to the difference in false positives and false negatives, we obtain:

$$||\text{SPRinT}_S \setminus \text{ON}_S| - |\text{ON}_S \setminus \text{SPRinT}_S|| = |\text{P}_S - \text{R}_S| \cdot s, \quad (25)$$

Thus, when $|\text{P}_S - \text{R}_S| \leq \epsilon$, it follows that:

$$||\text{SPRinT}_S \setminus \text{ON}_S| - |\text{ON}_S \setminus \text{SPRinT}_S|| \leq \epsilon s. \quad (26)$$

Finally, we obtain the probability bound for $|\widetilde{\text{PCT}}_S - \text{PCT}_S|$:

$$\Pr \left[|\widetilde{\text{PCT}}_S - \text{PCT}_S| \leq \epsilon \right] \geq 1 - \alpha, \quad (27)$$

holds provided the pilot sample size satisfies:

$$s_p \geq \frac{2 \ln(4/(\alpha + 1))}{(\epsilon - \omega_C)^2}. \quad (28)$$

With two bounds in Eq. 19 and 28, we establish Theorem 2. \square

3.4 Extensibility of the Framework

Our SPRinT framework accommodates various aggregation functions. The theoretical analysis developed for AVG and PCT can be extended to other value- and count-based aggregation functions. This involves straightforward modifications to the final aggregation computation while retaining the same sampling-based framework. For example, going from AVG to SUM involves scaling the sum by the ratio of dataset to the sample size. The error bounds for SUM are derived similarly to AVG, and adjusted to account for the linear scaling factor. For VAR, additional steps are needed to compute the mean and squared deviations, with error bounds that combine the deviations in both terms. Despite these modifications, the sampling process, pilot sample selection, and precision-recall optimization strategies remain applicable across different aggregation functions.

Table 2: Datasets, oracle and proxy models

Datasets	Oracle	Proxy
Mimic-III, eICU	Physicians	LIG-Doctor[20]
Jigsaw	User Labels	GLiClass
Jackson	Mask R-CNN[12]	ResNet-50[13]

This demonstrates the flexibility and broad applicability of our framework across various aggregation functions.

We note that while our framework is applicable to many aggregation functions, its effectiveness is most evident in a subset of functions, such as AVG, PCT, SUM, and VAR. In particular, the approximation guarantees for AVG and PCT can extend directly to SUM and VAR. Functions like MIN and MAX, however, are excluded from our theoretical analysis due to their inherent sensitivity to the sampling process. Indeed, even a single outlier in the sample can drastically alter the results, making sampling less reliable.

4 EXPERIMENTS

The purpose of our experiments is to evaluate our solution to AQNN queries w.r.t. objectives (O1) and (O2): error and cost. In § 4.1, we introduce the datasets, baselines, and evaluation measures. § 4.2 evaluates the effectiveness of SPRinT-V and SPRinT-C in minimizing aggregation error, as well as the impact of key parameters including $F\beta$ score, equalizing precision and recall, and radius r on the aggregation error. § 4.3 examines the efficiency of our methods w.r.t. execution time and scalability. Finally, in § 4.4, we demonstrate the application of AQNNs in hypothesis testing.

4.1 Experimental Setup

4.1.1 Datasets. We used datasets in three different domains.

Medical: MIMIC-III [19] and eICU [30] are publicly available clinical datasets containing de-identified data for patient stays across intensive care units (ICUs) in the United States. We adopt LIG-Doctor [20] to learn each patient’s embeddings from patient’s ICU admissions and regard the physician’s diagnoses as the oracle embeddings. The dataset has several patient attributes, including demographics (e.g., age, weight, height) and physiological measurements (e.g., blood pressure, hemoglobin levels), which are a rich source of AQNNs in medical contexts. After removing records with only one admission, the resulting MIMIC-III and eICU datasets contain 4,245 and 8,234 records respectively.

Social media: The Jigsaw Toxicity Classification Dataset (Jigsaw) [8] is a large-scale dataset containing user-generated comments labeled across multiple toxicity categories, including toxic, threat, and insult. We employ GLiClass, a zero-shot classifier, to learn comment embeddings, while the annotated toxicity labels serve as the oracle embeddings. To enhance the dataset for AQNN queries in social media, we synthesize additional attributes, such as the number of down-votes, to capture engagement dynamics. After preprocessing, we filter out non-toxic comments, resulting in a final dataset of 16,225 toxic comments.

Video: The Jackson dataset [6] is a real-world camera feed dataset capturing urban environments. Each frame is labeled with a boolean

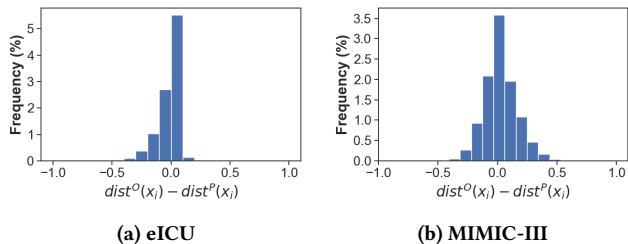


Figure 4: Distribution of the difference between proxy and oracle distances

value indicating the presence or absence of cars. We synthesize relevant attributes, like car speed. For our experiments, we uniformly sample 10,000 frames from the original 60,000-frame dataset.

The proxy and oracle models used for each dataset are shown in Table 2. The choices are justified by our analysis of sample complexity and pilot sample complexity in § 4.2.4.

4.1.2 Baselines. SPRinT supports AQNN approximation at a low cost and with low error as our experiments will show, and to our knowledge, is the first framework to do so. As such, there are no directly comparable frameworks. Given this, we evaluate SPRinT by comparing its effectiveness with the following approximate nearest neighbor search algorithms:

PQE-PT and PQE-RT. PQE-PT and PQE-RT are approximate FRNN query algorithms designed to pick nearest neighbors with minimal oracle usage while achieving predefined precision or recall targets, respectively, with high probability [10]. These solutions do not require any assumption about the proxy quality but calibrate the correlation between the oracle and the proxy by incurring some oracle calls. Specifically, a sample of objects in D is drawn to estimate the correlation between oracle and proxy distances for nearest neighbor selection. PQE-PT [10] is used as a sub-routine of SPRinT-V and SPRinT-C, although it only focuses on optimizing a single measure, precision. By default, we set the recall and precision targets to 0.95, as suggested in [10].

SUPG-PT and SUPG-RT. SUPG-PT and SUPG-RT transform an FRNN query into a binary classification problem, predicting whether a candidate object lies within a query radius r using proxy distances as predictors [23]. Given a query object q and a radius r , the FRNN query becomes: “For each object x , is it a neighbor of q within distance r ?” SUPG-PT and SUPG-RT use the proxy model P to output a high score when x is a likely nearest neighbor, and the oracle model O for validation, where $O(x) = 1$ indicates x is a true nearest neighbor. By combining proxy predictions with selective oracle validation, SUPG-PT and SUPG-RT ensure that the final query results meet predefined statistical guarantees for precision or recall, respectively.

Top-K. Probabilistic Top-K approximates nearest neighbors by returning the top- K nearest objects to the query, based on statistical guarantees from oracle predictions [25]. We map the Top-K query directly from the FRNN query, by setting K to the number of neighbors of q within radius r . Top-K relies on distributional assumptions over oracle predictions, which hold in many real-world scenarios, as

Table 3: Default number of oracle and proxy calls.

	eICU	MIMIC-III	Jigsaw	Jackson
C_P	1000	500	1000	1000
C_O	600	150	600	600

shown in Fig. 4, where $dist^X(x_i)$ represents the distance computed by X embeddings between x_i and q , with $X \in \{O, P\}$.

4.1.3 Evaluation Measures.

F β score is used to assess whether the true nearest neighbors have been identified by balancing precision and recall. It is defined as:

$$F\beta = (1 + \beta^2) \frac{PR}{\beta^2P + R} \quad (29)$$

where β is a positive real factor. Two commonly used values for β are 2 which weights recall higher than precision, and 0.5, which weights recall lower than precision.

Relative Error (RE) measures the deviation of the estimated aggregate from the ground truth, calculated as:

$$RE = \frac{|\widehat{\text{agg}_S} - \text{agg}_D|}{|\text{agg}_D|} \times 100\% \quad (30)$$

Cost represents the overall time and resources required for answering an AQNN, accounting for both (i) the number of oracle and proxy calls made, denoted by C_O and C_P respectively, and (ii) the execution time to evaluate the AQNN, given the corresponding embeddings. Each oracle call is at least one order of magnitude more expensive than a proxy call in terms of time, computational resources, or monetary cost. Hence, the total cost is significantly affected by C_O .

4.1.4 Default Parameters. We conduct experiments on the aggregate functions AVG, PCT, SUM, and VAR. To ensure a fair comparison with the baselines, we fix C_P and C_O as specified in Table 3. One exception is Top-K, which incurs oracle costs *dynamically* rather than using predefined values. Therefore, when comparing our algorithms with Top-K, we use the proxy cost from Table 3 but set the oracle cost to match Top-K’s incurred oracle cost.

To better illustrate algorithm effectiveness in answering AQNNs, we modify the attribute values of the true nearest neighbors so that their aggregates stand out from those computed on the global dataset. Specifically, half of the values are generated by bootstrap resampling from the nearest neighbor attribute value distribution with added noise (small standard deviation), while the other half are generated by bootstrap resampling from the global attribute value distribution with added noise (larger standard deviation). To maintain valid attribute ranges, we enforce dataset-specific clipping and shuffle the values to eliminate order bias.

Moreover, guided by empirical findings in Fig. 5, we set $\beta = 0.5$ for AVG, $\beta = 2$ for VAR and $\beta = 1$ for SUM. For PCT, SPRinT-C equalizes precision and recall so that β is irrelevant to nearest neighbor selection. We conduct experiments 30 times, as guided by the Central Limit Theorem (CLT), which ensures that the sample mean distribution approximates normality [24]. All reported measures are averaged over 10 random queries, with the target query q varying across runs to account for query-specific variability.

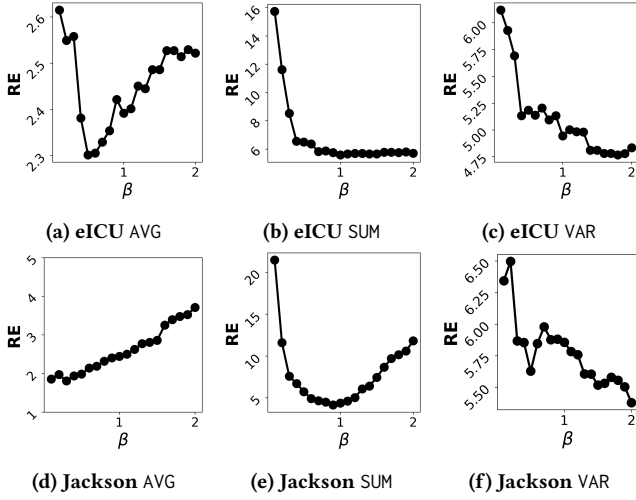


Figure 5: Impact of the values of β to RE.

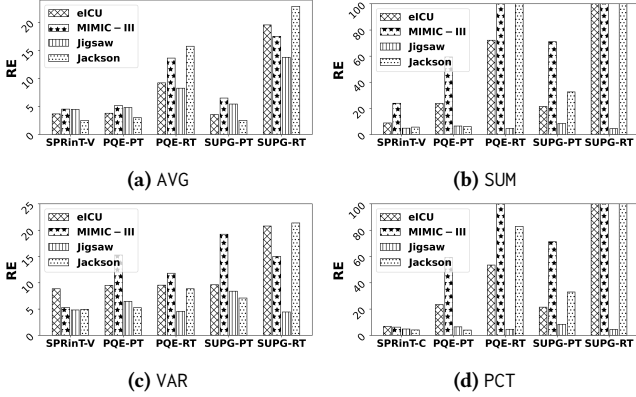


Figure 6: RE when aggregation function is AVG (a), SUM (b), VAR (c) or PCT (d).

4.2 Examining Aggregation Error

4.2.1 Relative Error Performance. Fig. 6 shows the RE performance of SPRinT-V for AVG, SUM, and VAR, as well as SPRinT-C for PCT across different datasets. We set a cut-off of 100 on RE.

SPRinT-V consistently achieves the lowest RE for all datasets across all baselines for AVG, SUM, and VAR in Fig. 6a, 6b, and 6c, respectively. For AVG, which is a normalized statistic, missing a few neighbors has a limited impact, making the advantage of our method relatively less pronounced. However, for SUM and VAR, where both precision and recall are critical, SPRinT-V’s performance demonstrates the effectiveness of our approach in achieving both.

In Fig. 6d, SPRinT-C also consistently achieves the lowest RE, demonstrating that our strategy of balancing precision and recall is effective in maintaining the number of nearest neighbors, which is crucial for count-based aggregation functions.

Unlike the above-mentioned algorithms, which operate under a predefined oracle budget, Top-K incurs oracle calls while searching for the nearest neighbors for $K = ON_S$. Thus, to ensure a fair

Table 4: RE of SPRinT-V and Top-K for AVG

	SPRinT-V			Top-K		
	RE	Time (s)	C_O	RE	Time (s)	C_O
eICU	3.34	1.33	991	3.33	73.88	991
MIMIC-III	3.17	0.51	496	3.23	5.72	496
Jigsaw	3.64	0.21	995	3.61	6.92	995
Jackson	2.01	1.77	994	2.00	13.72	994

Table 5: RE of SPRinT-C and Top-K for PCT

	SPRinT-C			Top-K		
	RE	Time (s)	C_O	RE	Time (s)	C_O
eICU	6.17	0.10	991	6.15	74.31	991
MIMIC-III	7.25	0.04	496	5.67	5.69	496
Jigsaw	2.49	0.09	995	2.49	6.75	995
Jackson	3.55	0.20	994	3.56	14.00	994

comparison, we evaluate SPRinT-V (resp. SPRinT-C) independently with Top-K by matching the pilot sample size to Top-K’s incurred oracle calls, and then compare the RE, execution time, and oracle calls (C_O) for AVG (resp. PCT) in Table 4 (resp. 5). SPRinT-V and SPRinT-C achieves nearly the same RE as Top-K with a consistent speedup of roughly 7-746x. For example, on eICU, SPRinT-V completes in 1.33s with RE of 3.34, compared to Top-K’s 73.88s and RE of 3.33.

4.2.2 Impact of $F\beta$ Score. For value-based aggregation functions, $F\beta$ score provides valuable insights into the RE performance. Table 6 reports the $F\beta$ scores achieved by SPRinT-V and baselines³.

SPRinT-V ranks the highest across all datasets, explaining its superior RE performance. However, a higher $F\beta$ score does not always lead to a lower RE for all value-based aggregation functions. For instance, on Jigsaw, although PQE-RT achieves a higher $F\beta$ score than PQE-PT, it results in worse RE performance for AVG as shown in Fig. 6a. This discrepancy arises because the $F\beta$ score measures set interaction (precision and recall) but does not account for the distribution of attribute values among the selected nearest neighbors. Consequently, false positives with extreme attribute values or the omission of similar false negatives can significantly impact the aggregate, leading to higher RE despite a high $F\beta$ score. Nonetheless, in scenarios where the distribution of nearest neighbor attribute values is unknown a priori, maximizing the $F\beta$ score remains the most effective strategy for reducing RE.

To further illustrate the effectiveness of SPRinT-V in identifying the optimal t^* which maximizes $F\beta$ score, we present two representative cases from the eICU and Jackson datasets, as shown in Fig. 7. We observe that the value of t corresponding to the peak of the $F\beta$ score curve is successfully identified as t^* by SPRinT-V.

4.2.3 Impact of Equalizing Precision and Recall. For count-based aggregation functions, such as PCT, the absolute difference between precision and recall in S achieved by each algorithm effectively explains their RE performance. Table 7 reports this absolute difference for SPRinT-C and baselines. SPRinT-C consistently achieves the lowest precision-recall difference for all datasets, which justifies its superior RE performance.

³Top performance in bold in Tables 6 - 9.

Table 6: $F\beta_S$ achieved by SPRinT-V

	SPRinT-V	PQE-PT	PQE-RT	SUPG-PT	SUPG-RT
eICU	0.959	0.936	0.797	0.951	0.497
MIMIC-III	0.792	0.699	0.494	0.665	0.379
Jigsaw	0.911	0.567	0.807	0.815	0.657
Jackson	0.943	0.928	0.600	0.909	0.382

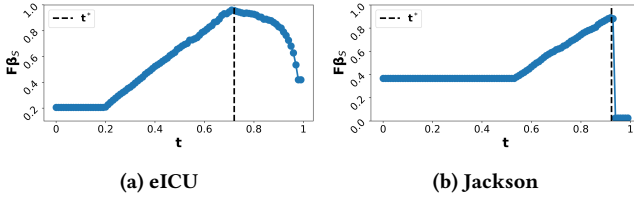


Figure 7: $F\beta$ score curves for eICU (a) and Jackson (b) datasets

Table 7: $|P_S - R_S|$ achieved by SPRinT-C

	SPRinT-C	PQE-PT	PQE-RT	SUPG-PT	SUPG-RT
eICU	0.021	0.208	0.216	0.182	0.511
MIMIC-III	0.042	0.552	0.499	0.709	0.666
Jigsaw	0.019	0.580	0.219	0.533	0.377
Jackson	0.019	0.024	0.451	0.329	0.661

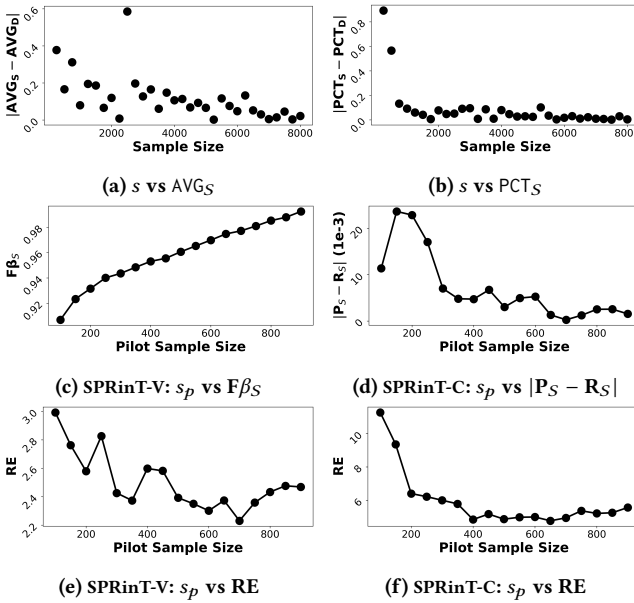


Figure 8: Impact of s_p and s of SPRinT for AVG (a, c, e) and PCT (b, d, f) using the eICU dataset.

4.2.4 Impact of Sample and Pilot Sample Complexity. In § 3, we present the minimum sample and pilot sample size required for a confidence interval of $(1 - \alpha)$. Here, we empirically illustrate their impact on RE for AVG (similar to SUM and VAR) and PCT using the eICU dataset in Fig. 8. For the pilot sample complexity analysis (Fig. 8c-8f), the sample size is fixed at 1000.

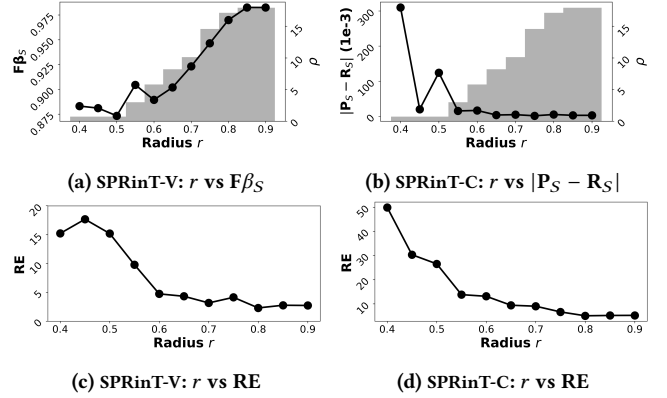


Figure 9: Impact of radius on the performance of SPRinT-V for AVG (a, c) and SPRinT-C for PCT (b, d) using the eICU dataset.

In Fig. 8a and 8b, as s increases, the aggregate in S converges toward the true aggregate in D . Larger sample sizes reduce sampling bias, leading to more accurate approximations of AQNNs in S . However, beyond a certain threshold (e.g., $s > 1000$ in Fig. 8b), the improvement diminishes.

Fig. 8c and 8e illustrate the impact of s_p using SPRinT-V. In Fig. 8c, increasing s_p consistently improves $F\beta_S$, which corresponds to the RE reduction observed in Fig. 8e. As discussed previously, a higher $F\beta$ score does not always lead to lower RE; however, we observe an overall decreasing trend. Fig. 8d and 8f show the impact of s_p using SPRinT-C. In Fig. 8d, the absolute difference between precision and recall in S decreases as s_p increases. Fig. 8f further illustrates the impact of equalizing precision and recall in S on RE. As s_p increases, RE decreases, stabilizing once s_p is sufficiently large. The initial rise in Fig. 8d occurs due to an insufficient number of nearest neighbors in the pilot sample, which prevents accurate monitoring of precision and recall in S . In other words, when s_p is too small, the optimal t^* for selecting nearest neighbors becomes unstable, leading to inconsistent neighbor selection across different runs. This variation introduces fluctuations in AQNN results, which in turn affect RE. Thus, our analysis aligns with the theoretical findings, indicating that a sufficiently large s_p is necessary for reliable monitoring of precision and recall in S .

We also ran experiments on Amazon retail datasets (not reported here due to space constraints) where nearest neighborhoods are highly sparse. As a result, the pilot sample yielded less reliable estimates of precision and recall. Our results corroborate that the poor estimation of t^* prevents SPRinT-V and SPRinT-C from consistently achieving lower RE. Interestingly, algorithms that prioritize precision, such as SUPG-PT and PQE-PT, exhibit better RE performance due to their conservative nearest neighbor selection strategy. This calls for developing adaptive strategies that account for sparsity in neighbor distributions, ensuring robust precision-recall balancing even in highly sparse settings.

4.2.5 Impact of Radius. Fig. 9 illustrates how varying r from 0.4 to 0.9 impacts the performance of SPRinT-V for AVG and SPRinT-C for PCT using the eICU dataset. As r increases, the true proportion of nearest neighbors, denoted by ρ , grows because more data points

Table 8: Time (sec) for AVG (similar as SUM, and VAR) AQNNs

	SPRinT	PQE-PT	PQE-RT	SUPG-PT	SUPG-RT	Top-K
eICU	0.95	0.94	0.90	0.95	0.81	0.95
MIMIC-III	0.07	0.03	0.02	0.02	0.02	5.72
Jigsaw	0.21	0.08	0.07	0.01	0.02	6.92
Jackson	0.35	0.07	0.09	0.02	0.03	13.72

Table 9: Time (sec) for PCT AQNNs

	SPRinT	PQE-PT	PQE-RT	SUPG-PT	SUPG-RT	Top-K
eICU	0.90	0.76	0.73	0.78	0.60	0.91
MIMIC-III	0.03	0.03	0.03	0.02	0.02	5.69
Jigsaw	0.11	0.09	0.08	0.02	0.02	6.75
Jackson	0.19	0.07	0.09	0.02	0.02	14.00

are included in the set of nearest neighbors. The values of ρ are visualized as bars in Fig. 9a and 9b, with the y-axis on the right.

For SPRinT-V, Fig. 9a shows the impact of r on $F\beta_S$. $F\beta_S$ fluctuates when r is small but increases as r grows. Based on our analysis of pilot sample complexity, this initial fluctuation results from the scarcity of nearest neighbors when r is very small (e.g., $\rho \leq 5\%$). As r increases, $F\beta_S$ becomes more stable. The impact of $F\beta_S$ on RE is shown in Fig. 9c. For SPRinT-C, similarly, Fig. 9b shows that $|P_S - R_S|$ fluctuates before decreasing as r increases. Consequently, RE follows a decreasing pattern in 9d.

4.3 Examining Cost

4.3.1 Time. We compare the execution time of SPRinT-V and SPRinT-C with baselines, assuming all embeddings are precomputed. Tables 8 and 9 show the results for AVG (similar to SUM and VAR) and PCT.

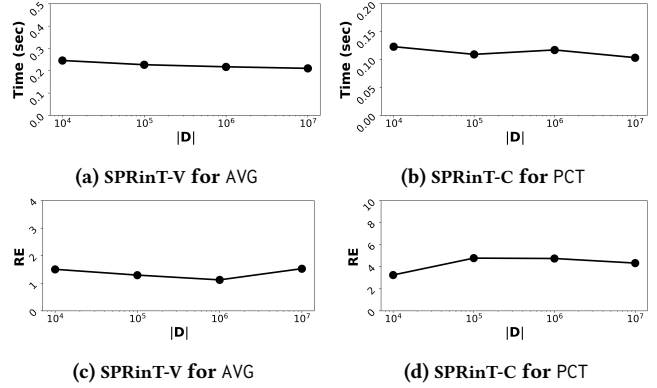
For AVG, SPRinT-V achieves competitive execution times across datasets. Given the algorithm’s complexity of $O(s^2)$, execution time increases quadratically with s , as observed in MIMIC-III and eICU where s increases from 500 to 1000. Notably, SPRinT-V is substantially faster than Top-K. Similarly, for PCT, SPRinT-C follows the same performance trends as the baselines.

4.3.2 Scalability. We evaluate the scalability of SPRinT-V and SPRinT-C using the semi-synthetic Jackson dataset. The original dataset is scaled from 10^4 to 10^7 , and we assess execution time and RE for AVG and PCT. We fix $(s$ and $s_p)$ at their default values in Fig. 10.

Fig. 10a and 10b show that the execution times for SPRinT-V and SPRinT-C remain stable as $|D|$ increases. Both theoretically and empirically, their execution time is independent of $|D|$. Also, Fig. 10c and 10d demonstrate that RE remains stable across different dataset sizes. Therefore, with sufficiently large s and s_p , the error performance of our proposed algorithms is also independent of $|D|$.

4.4 Application to Hypothesis Testing

AQNNs have a natural application in hypothesis testing because they provide aggregate statistics about the local neighborhood of a query object, which are crucial inputs for statistical inference. Hypothesis testing is a statistical method used to evaluate whether there is sufficient evidence in a sample to support or reject a specific claim about a population. When the population of interest is the neighborhood of a query object, this nearest neighbor hypothesis

**Figure 10: Impact of dataset size $|D|$ on the execution time and RE of SPRinT-V for AVG (a, c) and SPRinT-C for PCT (b, d) using Jackson dataset.**

(NNH) is made based on an AQNN. Hence, answering the AQNN is an essential intermediate step. Accurate testing of NNH can help practitioners uncover meaningful patterns, validate assumptions, and make reliable predictions. For example, it allows clinicians to determine whether the average blood pressure of patients similar to a given individual is significantly higher/lower than normal, guiding personalized treatment plans.

To evaluate SPRinT-V and SPRinT-C’s effectiveness in hypothesis testing, we perform one-sample t-tests and proportion z-tests, respectively. Both tests use a hypothesis of the form:

$$\text{agg}(\text{NN}_D(q, r)[\text{attr}]) \text{ op } c$$

where $\text{op} \in \{\leq, \geq, \neq\}$ and $c \in \mathbb{R}$ is a constant. Each hypothesis comes in pairs: a null hypothesis (H_0) and an alternative hypothesis (H_a). For instance, H_0 might state that “the average systolic blood pressure of patients similar to q equals 140 mmHg,” while H_a asserts that “the average is at most 140 mmHg.” To measure performance, we use **accuracy**, defined as the proportion of hypothesis testing results from approximate aggregates that match those derived from the true aggregate:

$$\text{Accuracy} = \frac{1}{k} \sum_{i=1}^k \mathbb{1}_{H(\text{agg}_D) = H(\text{agg}_S)}$$

where $k = 30$ is the number of samples. The constant c is set as a factor of the ground truth value, such that $c = \text{factor} \times \text{ground truth}$, ranging from 0.5 to 1.5 in steps of 0.05. Accuracy is averaged over 10 random queries and evaluated under two operators (\geq and \leq).

Fig. 11 demonstrates the accuracy of hypothesis testing across different datasets and algorithms. SPRinT-V and SPRinT-C consistently achieve the highest accuracy for t-tests and proportion z-tests (Fig. 11a and 11b, respectively). This is attributed to their accurate approximation of aggregates. The accuracy hovering around 0.5 imply that the algorithm cannot consistently determine whether the true aggregate supports the null or alternative hypothesis. Instead, their results appear to be random guesses between the two outcomes due to poor aggregate estimation. These results highlight that SPRinT-V and SPRinT-C are both cost-effective and efficient, enabling reliable and accurate testing of NNH for practical decision-making.

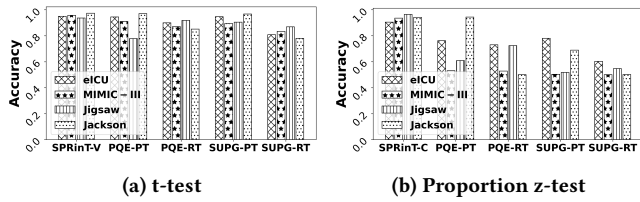


Figure 11: Hypothesis testing performance for AVG (a) and PCT (b) AQNNs.

5 RELATED WORK

5.1 Approximation Query Processing

Approximate Query Processing (AQP) methods aim to return approximate answers to Online Analytical Processing (OLAP) queries with high accuracy and low computational overhead. AQNNs differ from OLAP queries fundamentally in both scope and operation.

AQP techniques can generally be categorized into two types: online and offline. Online methods dynamically sample data at query time to compute approximate answers [1]. Offline methods, on the other hand, rely on precomputed synopses such as wavelets to answer queries efficiently [7]. Our method adopts a probabilistic top-k framework that distinguishes itself from these categories, which does not rely on precomputation nor does it dynamically sample data during query execution.

5.2 Nearest Neighbor Search

Nearest neighbor (NN) search methods can be categorized into exact and approximate approaches. Common methods, such as brute force, k-d trees, and cell techniques, are conceptually straightforward [4, 11]. However, these methods are impractical due to their high computational cost. Exact NN search typically relies on accurate embeddings generated by expensive oracle models and builds indexes over the entire database, leading to significant computational overhead [26].

As databases and data dimensionality grow, approximation algorithms are used to strike a balance between accuracy and efficiency. These approaches include hashing-based [15], tree-based [32], and index-based methods [3]. Additionally, [17] proposes a locality-sensitive hashing based approach and delivers sublinear query times and polynomial time processing costs, while [18] proposes space-efficient data structures guaranteeing compactness for Euclidean distances under specific accuracy constraints. FLANN [29] is a library leveraging randomized kd-trees and priority search k-means trees for scalable approximate NN finding over large datasets. Unlike our work, these approaches assume that the ground-truth representation of data objects is precomputed and can be efficiently accessed. The challenge in our problem is that the ground-truth representation needs to be computed on demand using expensive models. Recently, there has been a line of works relying cheap proxy models to approximate ground truth oracle labels and find accurate approximations of NN [21, 23, 25, 27]. For instance, Lai et al. propose probabilistic Top-K to train proxy models to generate oracle label distribution and output approximate Top-K solutions for video analytics [25]. In [23], the authors introduce statistical

accuracy guarantees, such as meeting a minimum precision or recall target with high probability, for approximate selection queries. Recently, Ding et al. introduce a framework for approximate queries that leverages proxy models to minimize the reliance on expensive oracle models [10]. They propose four algorithms to find high-quality answers for both precision-target and recall-target queries. However, these methods prioritize either precision or recall.

Notice that while SPRinT-V and SPRinT-C build upon PQE-PT, one of the algorithms proposed in [10], for selecting nearest neighbors, our work is substantially differentiated by two key aspects. First, PQE-PT assumes a *given* recall target as input and identifies neighbors that satisfy this target. In contrast, our algorithms *dynamically optimize both recall and precision targets*. Second, while PQE-PT focuses on maximizing recall given a precision target, SPRinT-V is designed to maximize the $F\beta$ score, and SPRinT-C aims to equalize recall and precision, which enable more accurate approximation of aggregates. Specifically, none of the algorithms in prior work including PQE-PT can achieve either of these objectives – max $F\beta$ score or equal precision and recall.

5.3 Post-ML-Inference Processing

General-purpose embeddings generated by machine learning models are typically trained on broader objectives, such as feature extraction or representation learning. These embeddings can be reused across various post-inference querying tasks, including anomaly detection [5], aggregation [9, 28], and nearest neighbor search [10, 23]. Our work leverages these embeddings as proxy models to facilitate a distinct task: the approximate answering of AQNNs.

6 CONCLUSION

We presented the SPRinT framework to address AQNNs, a new class of queries that compute an aggregate value over the predicted neighborhood of a given object. We showed that evaluating AQNNs exactly is expensive and proposed scalable algorithms that rely on sampling and a judicious combination of accurate oracle models and cheaper proxy models to efficiently approximate aggregates with low aggregation error. Our extensive experiments corroborate our theoretical analysis and strongly suggest that AQNNs can serve as a basis for important applications such as hypothesis testing.

Our future work includes the investigation of neighborhoods and the need for sparsity-aware sampling techniques as described in our experiments. Additionally, we are interested in evaluating AQNNs' applicability to two-sample hypothesis testing where the results of two AQNNs are compared. We believe our SPRinT framework could be extended to approximate such queries effectively.

REFERENCES

- [1] Sameer Agarwal, Barzan Mozafari, Aurojit Panda, Henry Milner, Samuel Madden, and Ion Stoica. 2013. BlinkDB: queries with bounded errors and bounded response times on very large data. In *Eighth Eurosys Conference 2013, EuroSys '13, Prague, Czech Republic, April 14-17, 2013*. ACM, 29–42. <https://doi.org/10.1145/2465351.2465355>
- [2] Michael R. Anderson, Michael J. Cafarella, Germán Ros, and Thomas F. Wenisch. 2019. Physical Representation-Based Predicate Optimization for a Visual Analytics Database. In *35th IEEE International Conference on Data Engineering, ICDE 2019, Macao, China, April 8-11, 2019*. IEEE, 1466–1477. <https://doi.org/10.1109/ICDE.2019.00132>
- [3] Akhil Arora, Sakshi Sinha, Piyush Kumar, and Arnab Bhattacharya. 2018. Hd-index: Pushing the scalability-accuracy boundary for approximate knn search in high-dimensional spaces. *arXiv preprint arXiv:1804.06829* (2018).

[4] Jon L Bentley. 1975. *A survey of techniques for fixed radius near neighbor searching*. Technical Report. Stanford, CA, USA.

[5] Markus M. Breunig, Hans-Peter Kriegel, Raymond T. Ng, and Jörg Sander. 2000. LOF: Identifying Density-Based Local Outliers. In *Proceedings of the 2000 ACM SIGMOD International Conference on Management of Data, May 16-18, 2000, Dallas, Texas, USA*. ACM, 93–104. <https://doi.org/10.1145/342009.335388>

[6] Christopher Canel, Thomas Kim, Giulio Zhou, Conglong Li, Hyeontaek Lim, David G. Andersen, Michael Kaminsky, and Subramanya Dullloor. 2019. Scaling Video Analytics on Constrained Edge Nodes. In *Proceedings of the Second Conference on Machine Learning and Systems, SysML 2019, Stanford, CA, USA, March 31 - April 2, 2019*. mlsys.org.

[7] Kaushik Chakrabarti, Minos N. Garofalakis, Rajeev Rastogi, and Kyuseok Shim. 2000. Approximate Query Processing Using Wavelets. In *VLDB 2000, Proceedings of 26th International Conference on Very Large Data Bases, September 10-14, 2000, Cairo, Egypt*. Morgan Kaufmann, 111–122. <http://www.vldb.org/conf/2000/P111.pdf>

[8] cjadams, Jeffrey Sorensen, Julia Elliott, Lucas Dixon, Mark McDonald, nithum, and Will Cukierski. 2017. Toxic Comment Classification Challenge. <https://kaggle.com/competitions/jigsaw-toxic-comment-classification-challenge>

[9] Jacob Devlin, Ming-Wei Chang, Kenton Lee, and Kristina Toutanova. 2019. BERT: Pre-training of Deep Bidirectional Transformers for Language Understanding. In *Proceedings of the 2019 Conference of the North American Chapter of the Association for Computational Linguistics: Human Language Technologies, NAACL-HLT 2019, Minneapolis, MN, USA, June 2-7, 2019, Volume 1 (Long and Short Papers)*. Association for Computational Linguistics, 4171–4186. <https://doi.org/10.18653/v1/N19-1423>

[10] Dujan Ding, Sihem Amer-Yahia, and Laks V. S. Lakshmanan. 2022. On Efficient Approximate Queries over Machine Learning Models. *Proc. VLDB Endow.* 16, 4 (2022), 918–931. <https://doi.org/10.14778/3574245.3574273>

[11] Jerome H. Friedman, Jon Louis Bentley, and Raphael A. Finkel. 1977. An Algorithm for Finding Best Matches in Logarithmic Expected Time. *ACM Trans. Math. Softw.* 3, 3 (1977), 209–226. <https://doi.org/10.1145/355744.355745>

[12] Kaiming He, Georgia Gkioxari, Piotr Dollár, and Ross B. Girshick. 2017. Mask R-CNN. In *IEEE International Conference on Computer Vision, ICCV 2017, Venice, Italy, October 22-29, 2017*. IEEE Computer Society, 2980–2988. <https://doi.org/10.1109/ICCV.2017.322>

[13] Kaiming He, Xiangyu Zhang, Shaoqing Ren, and Jian Sun. 2016. Deep Residual Learning for Image Recognition. In *2016 IEEE Conference on Computer Vision and Pattern Recognition, CVPR 2016, Las Vegas, NV, USA, June 27-30, 2016*. IEEE Computer Society, 770–778. <https://doi.org/10.1109/CVPR.2016.90>

[14] Wassily Hoeffding. 1994. Probability inequalities for sums of bounded random variables. *The collected works of Wassily Hoeffding* (1994), 409–426.

[15] Qiang Huang, Jianlin Feng, Yikai Zhang, Qiong Fang, and Wilfred Ng. 2015. Query-Aware Locality-Sensitive Hashing for Approximate Nearest Neighbor Search. *Proc. VLDB Endow.* 9, 1 (2015), 1–12. <https://doi.org/10.14778/2850469.2850470>

[16] Oliver Ibe. 2013. *Markov processes for stochastic modeling*. Newnes.

[17] Piotr Indyk and Rajeev Motwani. 1998. Approximate nearest neighbors: towards removing the curse of dimensionality. In *Proceedings of the thirtieth annual ACM symposium on Theory of computing*. 604–613.

[18] Piotr Indyk and Tal Wagner. 2018. Approximate nearest neighbors in limited space. In *Conference On Learning Theory*. PMLR, 2012–2036.

[19] Alistair EW Johnson, Tom J Pollard, Lu Shen, Li-wei H Lehman, Mengling Feng, Mohammad Ghassemi, Benjamin Moody, Peter Szolovits, Leo Anthony Celi, and Roger G Mark. 2016. MIMIC-III, a freely accessible critical care database. *Scientific data* 3, 1 (2016), 1–9.

[20] José F. Rodrigues Jr., Marco A. Gutierrez, Gabriel Spadon, Bruno Brandoli, and Sihem Amer-Yahia. 2021. LIG-Doctor: Efficient patient trajectory prediction using bidirectional minimal gated-recurrent networks. *Inf. Sci.* 545 (2021), 813–827. <https://doi.org/10.1016/j.ins.2020.09.024>

[21] Daniel Kang, John Emmons, Firas Abuzaid, Peter Bailis, and Matei Zaharia. 2017. NoScope: Optimizing Deep CNN-Based Queries over Video Streams at Scale. *Proc. VLDB Endow.* 10, 11 (2017), 1586–1597. <https://doi.org/10.14778/3137628.3137664>

[22] Daniel Kang, John Emmons, Firas Abuzaid, Peter Bailis, and Matei Zaharia. 2017. Noscope: optimizing neural network queries over video at scale. *arXiv preprint arXiv:1703.02529* (2017).

[23] Daniel Kang, Edward Gan, Peter Bailis, Tatsunori Hashimoto, and Matei Zaharia. 2020. Approximate Selection with Guarantees using Proxies. *Proc. VLDB Endow.* 13, 11 (2020), 1990–2003.

[24] Sang Gyu Kwak and Jong Hae Kim. 2017. Central limit theorem: the cornerstone of modern statistics. *Korean journal of anesthesiology* 70, 2 (2017), 144–156.

[25] Ziliang Lai, Chenxia Han, Chris Liu, Pengfei Zhang, Eric Lo, and Ben Kao. 2021. Top-K Deep Video Analytics: A Probabilistic Approach. In *SIGMOD '21: International Conference on Management of Data, Virtual Event, China, June 20-25, 2021*, Guoliang Li, Zhanhui Li, Stratos Idreos, and Divesh Srivastava (Eds.). ACM, 1037–1050. <https://doi.org/10.1145/3448016.3452786>

[26] Conglong Li, Minjia Zhang, David G. Andersen, and Yuxiong He. 2020. Improving Approximate Nearest Neighbor Search through Learned Adaptive Early

Termination. In *Proceedings of the 2020 International Conference on Management of Data, SIGMOD Conference 2020, online conference [Portland, OR, USA], June 14-19, 2020*. ACM, 2539–2554. <https://doi.org/10.1145/3318464.3380600>

[27] Yao Lu, Aakanksha Chowdhery, Srikanth Kandula, and Surajit Chaudhuri. 2018. Accelerating Machine Learning Inference with Probabilistic Predicates. In *Proceedings of the 2018 International Conference on Management of Data, SIGMOD Conference 2018, Houston, TX, USA, June 10-15, 2018*. ACM, 1493–1508. <https://doi.org/10.1145/3183713.3183751>

[28] Tomás Mikolov, Kai Chen, Greg Corrado, and Jeffrey Dean. 2013. Efficient Estimation of Word Representations in Vector Space. In *1st International Conference on Learning Representations, ICLR 2013, Scottsdale, Arizona, USA, May 2-4, 2013, Workshop Track Proceedings*, Yoshua Bengio and Yann LeCun (Eds.). <http://arxiv.org/abs/1301.3781>

[29] Marius Muja and David G Lowe. 2014. Scalable nearest neighbor algorithms for high dimensional data. *IEEE transactions on pattern analysis and machine intelligence* 36, 11 (2014), 2227–2240.

[30] Tom J Pollard, Alistair EW Johnson, Jesse D Raffa, Leo A Celi, Roger G Mark, and Omar Badawi. 2018. The eICU Collaborative Research Database, a freely available multi-center database for critical care research. *Scientific data* 5, 1 (2018), 1–13.

[31] Robert J Serfling. 1974. Probability inequalities for the sum in sampling without replacement. *The Annals of Statistics* (1974), 39–48.

[32] Chanop Silpa-Anan and Richard I. Hartley. 2008. Optimised KD-trees for fast image descriptor matching. In *2008 IEEE Computer Society Conference on Computer Vision and Pattern Recognition (CVPR 2008), 24-26 June 2008, Anchorage, Alaska, USA*. IEEE Computer Society. <https://doi.org/10.1109/CVPR.2008.4587638>

[33] Vivienne Sze, Yu-Hsin Chen, Tien-Ju Yang, and Joel S Emer. 2017. Efficient processing of deep neural networks: A tutorial and survey. *Proc. IEEE* 105, 12 (2017), 2295–2329.

7 APPENDIX

7.1 Bound for Precision and Recall in Pilot Sample

When the deviations between the proxy and oracle distances for different data points are i.i.d. random variables[10], each data point selected as a nearest neighbor by the proxy model has an independent and approximately uniform probability of being a true nearest neighbor according to the oracle. Hence, we let each data $x_i \in \text{SPRinT}_S \cap S_p$ be a Bernoulli random variable X_i , defined by:

$$X_i = \begin{cases} 1 & \text{if } x_i \in NN, \\ 0 & \text{otherwise.} \end{cases} \quad (31)$$

The precision in the pilot sample S_p can then be expressed as:

$$P_{S_p} = \frac{1}{|\text{SPRinT}_S \cap S_p|} \sum_{i=1}^{|\text{SPRinT}_S \cap S_p|} X_i. \quad (32)$$

Similarly, the precision in the entire sample S is given by:

$$P_S = \frac{1}{|\text{SPRinT}_S|} \sum_{i=1}^{|\text{SPRinT}_S|} X_i. \quad (33)$$

By Hoeffding’s inequality, the probability that the precision in S_p deviates from that in S by more than ω_{s_p} is bounded as follows:

$$\Pr \left[|P_{S_p} - P_S| \geq \omega_{s_p} \right] \leq 2 \exp \left(\frac{-2s_p \omega_{s_p}^2}{(b-a)^2} \right) = 2 \exp \left(-2s_p \omega_{s_p}^2 \right), \quad (34)$$

where $[a, b] = [0, 1]$ is the range of precision. With confidence level $(1 - \alpha)$, the minimal s_p is given by

$$s_p \geq \frac{\ln(2/\alpha)}{2\omega_{s_p}}. \quad (35)$$

The precision in S_p serves as a reliable approximation of the precision in S , with the probability of large deviations decreasing exponentially as s_p grows. We can derive a similar bound for recall.

If the deviations between the proxy and oracle distances for different data points are not i.i.d. random variables, the Bernoulli random variable assumption for each data point in $\text{SPRinT}_S \cap S_p$ no longer holds. Instead, we use Chebyshev's inequality [16], which only requires a finite variance, to provide a looser bound on the

probability of deviation between precision in S_p and S , as follows:

$$\Pr\left(|P_S - P_{S_p}| \geq \epsilon\right) \leq \frac{\text{Var}(P_{S_p})}{\epsilon^2}, \quad (36)$$

where $\text{Var}(P_{S_p})$ is the empirical variance of precision in S_p .

Although Chebyshev's inequality provides a less tight bound than Hoeffding's inequality, it allows us to control the deviations in precision and recall as s_p grows. By increasing s_p , the pilot sample better captures the distributional deviations in S , making precision and recall in S_p reliable estimates for those in S .